JACS
JOURNAL OF THE AMERICAN CHEMICAL SOCIETY
pubs.acs.org/JACS
Article

A Hydrometalation Initiation Mechanism via a Discrete Cobalt-Hydride for a Rapid and Controlled Radical Polymerization

Sajjad Dadashi-Silab and Erin E. Stache*

Cite This: J. Am. Chem. Soc. 2022, 144, 13311−13318
Read Online
ACCESS | Metrics & More | Article Recommendations | Supporting Information

ABSTRACT: Cobalt-mediated radical polymerization (CMRP) is a versatile technique for controlling the polymerization of vinyl monomers *via* reversible termination using Co^{II} complexes as persistent radical deactivators. Here, we report a facile approach for the *in situ* generation of Co−H as a discrete initiator and mediator for CMRP of acrylate and acrylamide monomers, overcoming the limitations of existing initiation strategies. *In situ* oxidation of a Co^{II} complex followed by transmetalation with silane generates a Co-H species, which initiates polymerization *via* hydrometalation of the monomer. This method precludes an induction period with excellent control over targeted molecular weight and dispersity. Strikingly, our approach allows complete polymerization when the induction period ends for conventional CMRP. A broad scope of monomers is amenable to this protocol, including acrylates and acrylamides. Tunable catalyst electronics afford tailored dispersity while maintaining agreement in molecular weight in stark contrast to conventional methods. Elimination of this induction period imbues polymerization behavior entirely to the catalyst electronic effects on reversible deactivation/activation rates.

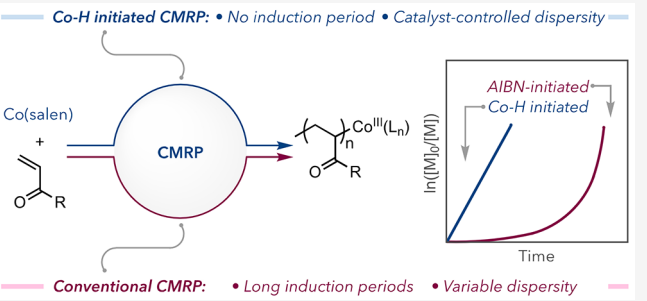

INTRODUCTION

Reversible deactivation radical polymerization (RDRP) techniques allow access to novel polymers by design and precise control of their molecular weight, dispersity, and other architectural properties.[1−7] In RDRP, reversible termination mechanisms include using persistent radicals such as alkoxyamines[8,9] or metal complexes[10,11] to mediate polymer chain growth. In particular, cobalt-mediated radical polymerizations (CMRP) use cobalt(II) complexes as persistent radicals to deactivate propagating radicals and assert control over polymerization.[12−18] In CMRP, dormant polymer chains contain organocobalt end groups, which can reversibly dissociate to generate propagating radicals and Co^{II} complexes as polymerization deactivators. In addition, the CMRP equilibrium can be tuned by the identity of the Co^{II} complex, modifying the strength of the cobalt−carbon bond.

Initiation in conventional CMRP proceeds with exogenous radical sources, generating organocobalt(III) complexes *in situ* and showing long induction periods (Scheme 1A).[19−21] Moreover, a large excess of exogenous initiators must be used to achieve a reasonable polymerization rate. As a result, continuous generation of an initiating species forms new chains throughout the polymerization, broadening molecular weight distribution. Presynthesized organocobalt compounds have been used as discrete initiators in CMRP.[22−26] However, the synthesis of organocobalt compounds often brings additional synthetic challenges, requiring the reaction of Co^{II} with radicals pre-polymerization.

We envisioned a new approach utilizing Co−H as a discrete initiator in CMRP. Inspired by the Mukaiyama hydration of alkenes[27] and implementation of this approach by Shenvi and others (Scheme 1B),[28−30] our design relies on the oxidation of a Co^{II}(salen) complex to Co^{III} followed by transmetalation with a hydrosilane to generate a Co−H initiator *in situ* (Scheme 1C). The Co−H species will rapidly initiate polymerization by hydrometalation of vinyl monomers, whereby CMRP equilibrium solely exerts control. This approach would preclude exogenous initiators and synthesis of organocobalt complexes and should eliminate the long induction period typically observed in CMRP.

The Co^{II}(salen) complex has been shown as a versatile persistent radical in CMRP, affording controlled polymerization with several monomer classes and also used in hydrometalation reactions. Judicious choices of oxidant, silane, and stoichiometry are essential for a well-controlled polymerization. The oxidation of Co^{II}(salen) to Co^{III}(salen)-X (or $[Co^{III}(salen)]^+$) must occur rapidly, be tolerant of monomer, and not inhibit polymerization. The transmetalation with silane must also be highly efficient and rapid to ensure initiator formation. Finally, hydrometalation

Received: April 30, 2022
Published: July 14, 2022

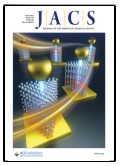

https://doi.org/10.1021/jacs.2c04655
J. Am. Chem. Soc. 2022, 144, 13311−13318

Scheme 1. Approaches in the Initiation of Cobalt-Mediated Radical Polymerization (CMRP)[a]

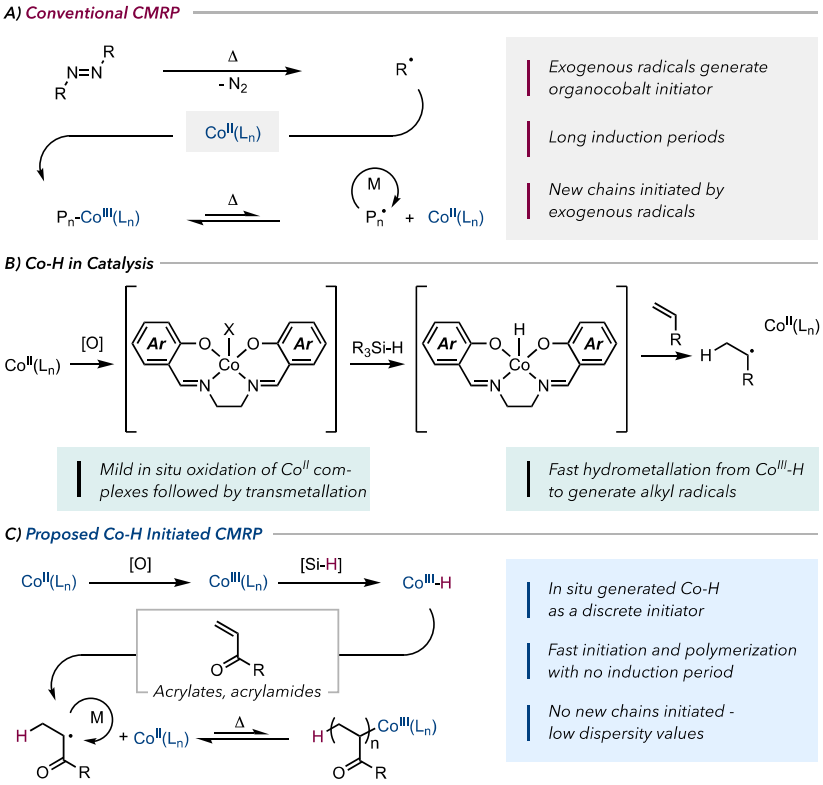

[a](A) Conventional CMRP using exogenous radical sources to generate the organocobalt initiators. (B) Inspiration using Co−H in catalytic alkene hydration. (C) Proposed *in situ* generation of Co−H species as a fast and efficient initiator for mediating the CMRP of acrylate and acrylamide monomers.

must be nearly instantaneous for fast initiation and to prevent catalyst deactivation by conversion of Co^{III}−H to Co^{II} and H_2. All these steps can be influenced by the choice of salen ligand in addition to the oxidant and silane. Modifying the salen ligand can further provide opportunities for tuning the Co complexes' structural properties and polymerization efficiency.

RESULTS AND DISCUSSION

We began our studies with the CMRP of methyl acrylate (MA) monomer with these design principles in mind. The Co^{II}(salen) complex was oxidized to Co^{III} by *N*-fluoro-2,4,6-trimethylpyridinium tetrafluoroborate (NFTPB) followed by the addition of 1,1,3,3-tetramethyldisiloxane (TMDSi) to generate the Co−H initiator *in situ* (Figure S1). Polymerization of MA in *N*,*N*-dimethylformamide (DMF) reached 85% monomer conversion with a low dispersity of 1.09 and molecular weight in agreement with theoretical value (I_{eff}, 104%; Table 1, entry 1, and Figure S3). Excluding either the Co complex, oxidant, or silane showed no monomer conversion (Table S1), confirming the importance of the oxidant and silane in generating the Co−H initiator. Polymerization of MA using **Co1** and TMDSi was also well controlled in other solvents such as toluene, dioxane, acetonitrile, *N*,*N*-dimethylacetamide (DMAc), and dimethyl sulfoxide (DMSO) or even in bulk conditions (Figure S5). Using strongly coordinating solvents (DMF, DMAc, and DMSO) resulted in increased monomer conversion than those with less coordinating ability such as toluene.

The use of phenylsilane ($PhSiH_3$) in place of TMDSi also afforded low dispersity, albeit with lower initiator efficiency (Table 1, entry 2). Decreasing the concentration of TMDSi, which contains two Si−H functionalities, from 0.5 to 0.25 equiv (with respect to **Co1**) showed a decrease in the initiator efficiency from 104 to 49%, while the use of excess silane increased the initiator efficiency, suggesting the formation of new chains (Table 1, entries 3 and 4, and Figure S6). Using 0.25 equiv of the oxidant and silane (with respect to Co), which would result in the oxidation and transmetalation of ∼50% of the initial **Co1**, polymerization of MA showed an initiator efficiency of ∼61% (Table 1, entry 5). However, a high concentration of **Co1** as the deactivator of propagating radicals significantly decreased the polymerization rate, reaching only 8% monomer conversion in 24 h. In the presence of excess oxidant and silane, initiator efficiencies higher than 100% were achieved, suggesting the formation of additional new chains (Table 1, entry 6).

To support our hypothesis of a radical mechanism, a control experiment conducted in the presence of TEMPO as a radical scavenger showed no monomer conversion after 24 h (Table 1, entry 7). Moreover, the addition of TEMPO after the reaction was started (t = 15 min) completely stopped the polymerization with no further monomer conversion or molecular weight increase (Table 1, entry 8). These control experiments further indicate the radical nature of the initiation and polymerization by Co−H. We were also able to synthesize high molecular weight polymers (M_n > 50,000 g/mol) by targeting high degrees of polymerization (DP). The CMRP of MA was well controlled, targeting a DP of 400, 600, or 800, resulting in high initiator efficiency, low dispersity, and narrow molecular weight distributions (Table 1, entries 9−11, and Figure S7).

Kinetic analysis of our protocol compared to typical CMRP protocols shows a stark contrast in both induction period and

https://doi.org/10.1021/jacs.2c04655
J. Am. Chem. Soc. 2022, 144, 13311−13318

Table 1. Co−H-Initiated CMRP of Methyl Acrylate (MA)[a]

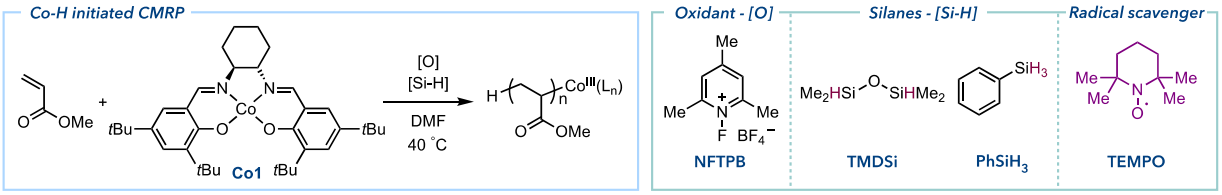

entry	[MA]/[**Co1**]/[O]/[Si−H]	conversion (%)	$M_{n,th}$ (g/mol)	M_n (g/mol)	$Đ$	I_{eff} (%)[b]
1	200/1/0.55/0.5	85	15,200	14,500	1.09	104
2[c]	200/1/0.55/0.33	62	11,300	15,300	1.11	74
3	200/1/0.55/0.25	53	9750	20,000	1.09	49
4	200/1/0.55/1	78	14,000	10,250	1.17	137
5[d]	200/1/0.25/0.25	8	1970	3200	1.09	61
6	200/1/0.75/0.75	95	16,900	12,500	1.20	135
7[e]	200/1/0.55/0.5 + TEMPO (added initially)	0				
8[f]	200/1/0.55/0.5 + TEMPO (added at 15 min)	17	3500	3150	1.11	111
9	400/1/0.55/0.5	86	30,100	24,300	1.12	123
10	600/1/0.55/0.5	85	44,400	36,500	1.23	121
11	800/1/0.55/0.5	86	59,800	50,300	1.26	118

[a]Oxidant, [O] = *N*-fluoro-2,4,6-trimethylpyridinium tetrafluoroborate (NFTPB), [Si−H] = 1,1,3,3-tetramethyldisiloxane (TMDSi), reaction time = 2 h. [b]Initiator efficiency, $I_{eff} = (M_{n,th}/M_n)$. Theoretical number-average molecular weight, $M_{n,th} = ([MA]/[\mathbf{Co1}] \times \text{conversion} \times M_{MA}) + M_{Co(Ln)}$. [c][Si−H] = phenylsilane ($PhSiH_3$). [d]Oxidant used in 0.25 equiv with respect to Co. Reaction time = 24 h; no monomer conversion after 4 h. [e]TEMPO (1.5 equiv) with respect to **Co1** was added initially. [f]TEMPO (1.5 equiv) was added 15 min after polymerization was started; no further monomer conversion was observed after 4 h.

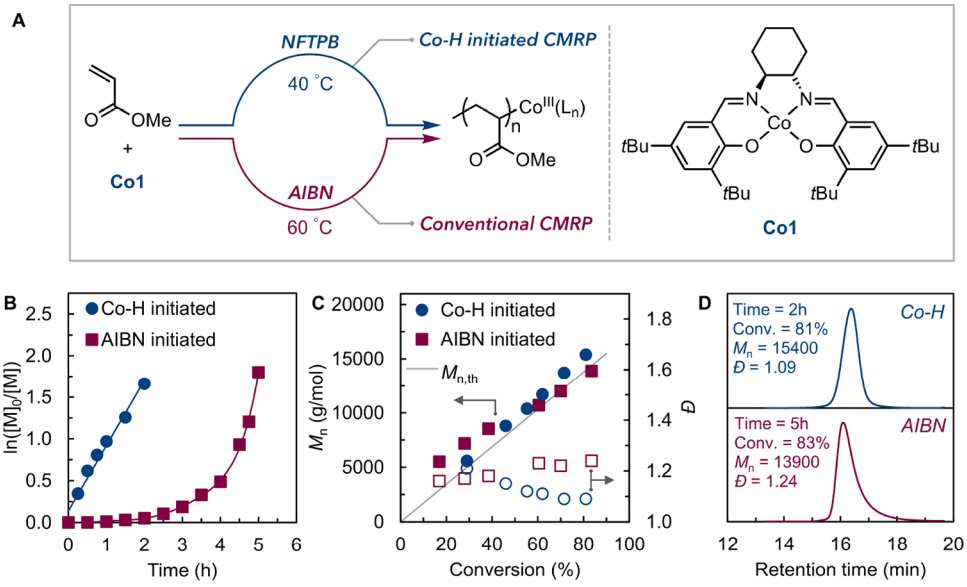

Figure 1. (A) CMRP of MA initiated by Co−H or AIBN. (B) Kinetics of the polymerization of MA showing an induction period in the presence of AIBN, whereas the Co−H-initiated system showed a fast and linear growth with no induction period. (C) Evolution of molecular weight (M_n, filled points, left *y* axis) and dispersity ($Đ$, open points, right *y* axis) per monomer conversion. (D) GPC traces of the resulting polymers. Reaction conditions for Co−H-initiated polymerization: [MA]/[**Co1**]/[NFTPB]/[TMDSi] = 200/1/0.55/0.5 in DMF (50 vol %) at 40 °C. Reaction conditions for AIBN initiated polymerization: [MA]/[**Co1**]/[AIBN] = 200/1/6 in DMF (50 vol %) at 60 °C.

polymerization control (Figure 1A). Our standard conditions show a linear semi-logarithmic kinetic behavior, reaching >80% monomer conversion in just 2 h (Figure 1B). Strikingly, under standard CMRP conditions using excess amounts of azobisisobutyronitrile (AIBN) as an exogenous radical source, polymerization of MA at 60 °C shows a long induction period (~3 h; Figure 1B).

The long induction period is typically expected as polymerization does not begin until the Co^{II} deactivator is depleted by coupling with exogenous radicals. Conducting polymerization of MA initiated by Co−H at 20 °C showed only negligible monomer conversion due to the slow Co−C bond activation rate at low temperatures. Increasing the temperature to 60 °C increased the polymerization rate with high monomer conversion, controlled molecular weights, and low dispersity (Figure S8).

In both protocols, molecular weights increased as a function of monomer conversion (Figure 1C). Co−H initiation affords polymer in agreement with theoretical values confirming quantitative initiator efficiency (Figure 1C). Furthermore, the

https://doi.org/10.1021/jacs.2c04655
J. Am. Chem. Soc. 2022, 144, 13311−13318

Table 2. Co−H-Initiated CMRP of Acrylate and Acrylamide Monomers[a]

	Acrylate monomers					*Acrylamide monomers*		
	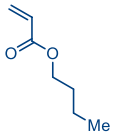	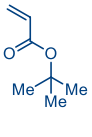	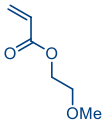	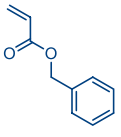	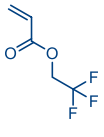		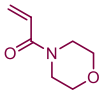	
	***n*-BA**	***t*-BA**	**MEA**	**BnA**	**TFEA**	**DMA**	**NAM**	**NiPAAm**
Conv. (%)	94	85	75	63	60	85	84	>99
$M_{n,th}$	24500	22400	20100	21000	19100	17500	24300	23300
M_n	21500	22000	16000	17000	19800	18000	24400	29000
$Đ$	1.18	1.12	1.09	1.09	1.13	1.06	1.18	1.26
I_{eff} (%)	114	98	125	123	96	97	99	80

[a]Reaction conditions: [M]/[**Co1**]/[NFTPB]/[TMDSi] = 200/1/0.55/0.5 in DMF (50 vol %) at 40 °C, 2 h; [NiPAAm] = 4 M in DMF (M_n and $M_{n,th}$ values are given in g/mol).

GPC traces showed a narrow, monomodal molecular weight distribution of the resulting polymer initiated by Co−H with a dispersity of 1.09 (Figure 1D, top). Polymerization of MA in the presence of excess AIBN and **Co1** shows molecular weights close to theoretical values as polymerization progresses to higher monomer conversions. However, the dispersity of the polymers also increases ($Đ$ > 1.24) because of the continuous generation of new radicals via AIBN decomposition. The GPC traces of the resulting polymer initiated by AIBN show tailing toward low molecular weights indicative of new chains generated throughout the polymerization (Figure 1D, bottom, and Figure S9).

Co−H-initiated CMRP was successfully applied in controlling the polymerization of various acrylate monomers (Table 2 and Figures S10−S17). Under our standard polymerization conditions, acrylate monomers such as *n*-butyl (*n*-BA), *t*-butyl (*t*-BA), 2-methoxyethyl (MEA), and benzyl (BnA) acrylate were polymerized in a controlled fashion using Co−H as the initiator and polymerization mediator. Polymerization of a fluorinated monomer, 2,2,2-trifluoroethyl acrylate (TFEA), reached ∼60% monomer conversion, providing a dispersity of 1.13 and initiator efficiency of 96%.

In addition, we were able to initiate and control the polymerization of acrylamide monomers using Co−H as the initiator and mediator. For example, *N*,*N*-dimethylacrylamide (DMA) was polymerized to high monomer conversion with controlled molecular weight (I_{eff} = 97%) and low dispersity ($Đ$ = 1.06). Furthermore, polymerization of *N*-acryloylmorpholine (NAM) was well-controlled using Co−H. As a secondary acrylamide monomer, the CMRP of *N*-isopropylacrylamide (NiPAAm) reached >99% monomer conversion and showed controlled molecular weight and low dispersity.

Polymerization of other monomers such as methyl methacrylate (MMA), styrene, or vinyl acetate (VOAc) failed to provide control via Co−H-initiated CMRP. Methacrylate monomers are known to undergo catalytic chain transfer in the presence of Co^{II} complexes, yielding alkene-terminated, low-molecular-weight polymers. The CMRP of MMA under the standard conditions of Co−H initiation showed 62% monomer conversion in 24 h with M_n = 1150 ($M_{n,th}$ = 13,000) and $Đ$ = 1.62 (Figure S18). Furthermore, polymerization of styrene resulted in only 12% monomer conversion with M_n = 7250 and $Đ$ = 2.07 (Figure S19). Although CMRP of VOAc initiated by AIBN provided only moderate control over the polymerization (with initiator efficiencies >200% as the polymerization progressed to ∼80% conversion; Figure S20), no monomer conversion was observed in the presence of Co−H. We hypothesize that due to its lower activity, the hydrometalation of VOAc is slow relative to the decomposition of Co−H to Co(II) and H_2.

In situ chain extension experiments confirmed the chain-end fidelity of polymers synthesized by Co−H-initiated CMRP (Figure 2). A poly(methyl acrylate) (PMA) macroinitiator was

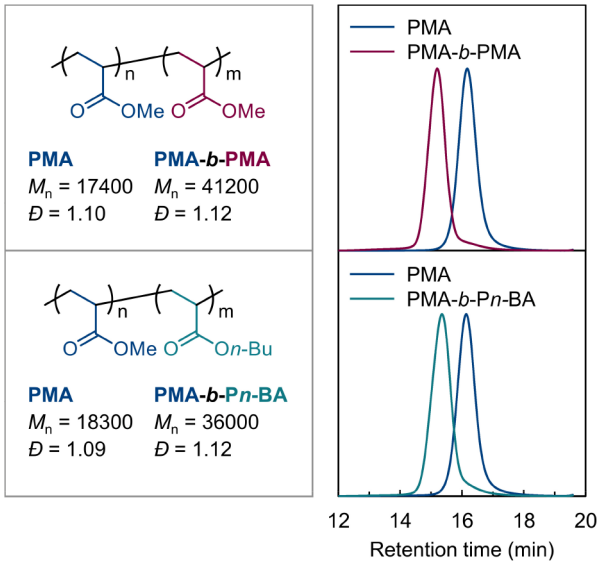

Figure 2. Results of chain extension experiments showing high chain-end fidelity of polymers initiated by Co−H (M_n values in g/mol).

initially synthesized, followed by the *in situ* addition of a second batch of MA monomer. As shown in Figure 2, GPC analysis of the polymers shows a shift toward higher molecular weights upon chain extension of the PMA macroinitiator without any significant dead chains observed in the GPC traces. The molecular weight of the polymer increased from 17,400 to 41,200, still showing a low dispersity of 1.12. Furthermore, we synthesized a block copolymer by chain extension of PMA macroinitiator by *n*-butyl acrylate (*n*-BA) monomer in a controlled manner.

Given the striking differences in polymerization kinetics based on the initiation mode, we sought to explore the polymerization efficiency as a function of the electronic properties through a series of salen ligands (Figure 3A). In the absence of any electron-withdrawing groups on the Co complex (*i.e.*, Co(salen-

https://doi.org/10.1021/jacs.2c04655
J. Am. Chem. Soc. 2022, 144, 13311−13318

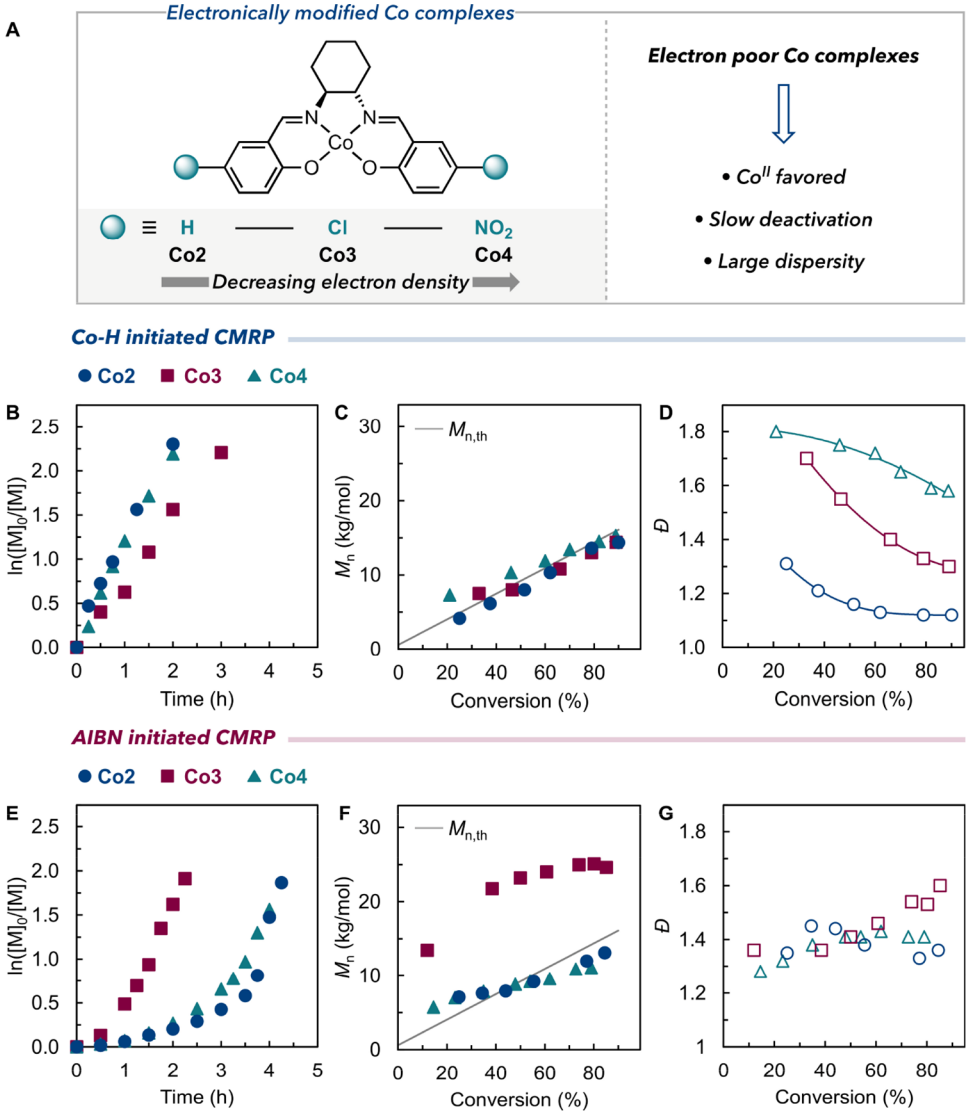

Figure 3. (A) CMRP of MA in the presence of Co(salen) complexes bearing H, Cl, and NO_2 substitutions. (B) Kinetics, (C) molecular weight (M_n), and (D) dispersity ($Đ$) of polymers in Co−H-initiated CMRP (lines are added to guide the eye); reaction conditions: [MA]/[$Co^{II}(L_n)$]/[NFTPB]/[TMDSi] = 200/1/0.55/0.5 in DMF (50 vol %) at 40 °C. (E) Kinetics, (F) molecular weight (M_n), and (G) dispersity ($Đ$) of polymers in AIBN-initiated CMRP; reaction conditions: [MA]/[$Co^{II}(L_n)$]/[AIBN] = 200/1/6 in DMF (50 vol %) at 60 °C.

H), **Co2**), the CMRP of MA was well controlled and showed molecular weights in agreement with theoretical values throughout the polymerization and low dispersity ($Đ \approx 1.1$).

In the presence of an electron-withdrawing group such as Cl or NO_2, the Co−H-initiated CMRP of MA results in polymers with high dispersity values ($Đ \approx 1.3-1.8$). With a Cl-substituted Co complex (*i.e.*, Co(salen-Cl), **Co3**), slightly higher dispersity polymers are obtained, finally reaching a dispersity of 1.3 but with controlled molecular weights. The deactivation efficiency of **Co3** with Cl substitutions appeared to be lower than **Co2** with no electron-withdrawing substitutions, providing slower deactivation of propagating chains and larger dispersity values.

With the **Co4** complex containing NO_2 substitutions, molecular weights were initially slightly higher than theoretical values, indicating slow initiation at the early stages of the polymerization (<20% monomer conversion). The slight initial discrepancy between the molecular weights could be attributed to the slow rate of oxidation/transmetalation with the electron-deficient Co(salen) complexes due to their increased oxidation potentials.[21,31] Nevertheless, high initiator efficiencies were achieved, and molecular weights reached theoretical values at high conversions. The resulting polymer showed high dispersity values, indicating a diminished rate of deactivation in the presence of NO_2-substituted Co(salen) complex. These results indicate that electron-withdrawing groups decrease the polymerization efficiency and deactivation rate of Co(salen) as electron-poor complexes would favor Co^{II} (active polymerization state) over Co^{III} (dormant polymerization state).

The *para*-substituted electronically modified Co(salen) complexes were also examined under conventional CMRP conditions in the presence of AIBN as the initiator (Figure 3). Kinetics of the polymerization of MA showed induction periods with all the three Co complexes. However, Co(salen-Cl) (**Co3**) showed the shortest induction period (<0.5 h), with monomer conversion reaching ~85% in 2.5 h (Figure 3E). In addition, the resulting polymer showed molecular weights significantly higher than theoretical values, indicating low initiator efficiency (I_{eff} < 60%) throughout the polymerization (Figure 3F).

Despite the lower electron density of Co(salen-NO_2) (**Co4**) than **Co3**, polymerization of MA with **Co4** showed a longer

https://doi.org/10.1021/jacs.2c04655
J. Am. Chem. Soc. 2022, 144, 13311−13318

Table 3. Co−H-Initiated CMRP of MA with Backbone-Modified Co(salen) Complexes Using Different Diamine Building Blocks[a]

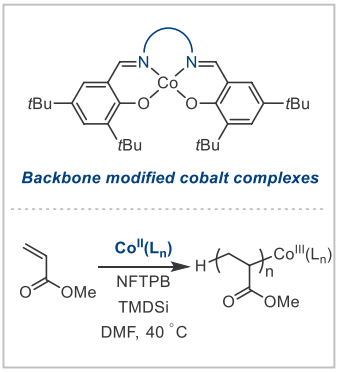

$Co^{II}(L_n)$:	Co1	Co5	Co6	Co7	Co8	Co9	Co10
Time (h)	2	2	2	0.5	0.5	2	0.5
Conv. (%)	85	80	83	96	70	63	80
$M_{n,th}$	15200	14300	14900	17200	12700	11500	14500
M_n	14500	14500	14400	28000	17000	12000	16500
$Đ$	1.09	1.18	1.11	1.53	1.49	1.14	1.15
I_{eff} (%)	104	99	103	62	74	96	88

[a]Reaction conditions: [MA]/[$Co^{II}(L_n)$]/[NFTPB]/[TMDSi] = 200/1/0.55/0.5 in DMF (50 vol %) at 40 °C (M_n and $M_{n,th}$ values are given in g/mol).

induction period (~2 h) and molecular weights close to theoretical values. Indeed, the CMRP of MA using **Co4** and Co(salen-H) (**Co2**) showed similar rates of polymerization and induction periods (~2 h) and control over molecular weight. We postulate that radicals generated from AIBN decomposition may interact with the NO_2 groups of the complex and decrease the concentration of radicals, resulting in a relatively longer induction period than with **Co3**. In contrast, AIBN-derived radicals can initiate the polymerization without efficient deactivation by the **Co3** complex. This data shows that using discrete Co−H initiators with nearly instantaneous initiation eliminates the induction period with exogenous radicals. Thus, polymerization behavior can be isolated to and almost entirely dictated by the role of complex electronics on reversible deactivation/activation rates. Furthermore, targeted molecular weights with desired dispersity (broad or narrow) are achievable using this protocol. In contrast, conventional initiation approaches afford more limited control over molecular weight and dispersity.

We further explored the effect of ligand structure on the CMRP of MA by changing the diamine backbone of the salen ligands under both Co−H and AIBN initiation approaches (Table 3). The Co−H-initiated polymerization of MA was well controlled using Co complexes that featured cyclohexane (**Co1**), ethylene (**Co5**), and 1,2-diphenyl-1,2-ethylenediamine (**Co6**) backbones. In the presence of these complexes, high monomer conversions were achieved with molecular weights close to theoretical values ($I_{eff} \approx 99-104\%$) and low dispersities. However, in the presence of a Co complex with a 1,3-diaminopropane (**Co7**) backbone, poor control over the polymerization was observed with a dispersity of 1.59 and an initiator efficiency of 67%. Furthermore, **Co7** also showed poor efficiency in controlling the polymerization of MA initiated by AIBN (Figure S34). In the presence of **Co7** and AIBN, the polymerization of MA reached >90% monomer conversion in <30 min with low initiator efficiency and a large dispersity of 3.04, indicating a lack of control provided by this complex.

The Co complex with a 1,2-phenylenediamine backbone (**Co8**) resulted in poor control over the polymerization of MA, showing high dispersity (1.47) and low initiator efficiency of 73% under Co−H initiation conditions. In the presence of AIBN, **Co8** also provided poor control over the polymerization of MA with molecular weights higher than theoretical values and large dispersities (Figure S35). Interestingly, using a 4,5-disubstituted phenylenediamine backbone with methyl (**Co9**) or bromo (**Co10**) substituents restored control over the polymerization of MA initiated by Co−H, showing controlled molecular weight with high initiator efficiency and low dispersity ($Đ \approx 1.15$). The AIBN-initiated CMRP of MA with **Co9** also proved its capability in controlling polymerization under conventional initiation approaches with quantitative initiator efficiencies and low dispersity values ($Đ \approx 1.15$) (Figure S35). We hypothesize that due to the conjugated nature of the ligand, the phenylene backbone **Co8** is susceptible for side reactions with radicals, receding its ability to afford controlled molecular weight and dispersity. Substitution of the phenylene backbone with methyl or Br groups prevents any side reactions and affords well-controlled CMRP. To further prove this hypothesis, we subjected **Co8** to react with AIBN prior to polymerization for any possible substitution of the phenylene backbone by radicals derived from AIBN. The *in situ* addition of MA and additional AIBN afforded well-controlled polymers with high initiator efficiency and low dispersity as observed in the presence of **Co9** with methyl substituents (Figure S35).

CONCLUSIONS

In summary, we have developed a fast and efficient approach for initiating and controlling a cobalt-mediated radical polymerization using Co−H as a discrete initiating species generated *in situ*. This system provides excellent control over the homo- and co-polymerization of various acrylate and acrylamide monomers. We demonstrated that Co−H-initiated polymerizations proved advantageous in offering fast kinetics and improved control over molecular weight and dispersity of the polymers instead of those initiated in the presence of exogenous initiators. Furthermore, the electronic properties of the Co(salen) complexes show a profound effect on their polymerization behavior, allowing further control of polymer properties such as dispersity. Under our protocol, electron-withdrawing substitutions resulted in tunable dispersity but controlled molecular weight, indicating the importance of deactivation rate in electron-deficient Co(salen) complexes.

ASSOCIATED CONTENT

Supporting Information

The Supporting Information is available free of charge at https://pubs.acs.org/doi/10.1021/jacs.2c04655.

https://doi.org/10.1021/jacs.2c04655
J. Am. Chem. Soc. 2022, 144, 13311−13318

Details of the experimental procedures and additional supplementary results (PDF)

AUTHOR INFORMATION

Corresponding Author

Erin E. Stache − *Department of Chemistry and Chemical Biology, Cornell University, Ithaca, New York 14853, United States;* orcid.org/0000-0002-4670-9117; Email: ees234@cornell.edu

Author

Sajjad Dadashi-Silab − *Department of Chemistry and Chemical Biology, Cornell University, Ithaca, New York 14853, United States;* orcid.org/0000-0002-4285-5846

Complete contact information is available at: https://pubs.acs.org/10.1021/jacs.2c04655

Notes

The authors declare no competing financial interest.

ACKNOWLEDGMENTS

Financial support provided by Cornell University. This work made use of the NMR Facility at Cornell University and is supported, in part, by the NSF under award CHE-1531632. This work made use of the Cornell Center for Materials Research Facilities supported by the National Science Foundation under award DMR-1719875. The authors acknowledge preliminary efforts by Jonathan Rowell and Steven K. Knauss.

REFERENCES

(1) Matyjaszewski, K. Atom Transfer Radical Polymerization (ATRP): Current Status and Future Perspectives. *Macromolecules* **2012**, *45*, 4015−4039.

(2) Perrier, S. 50th Anniversary Perspective: RAFT Polymerization—A User Guide. *Macromolecules* **2017**, *50*, 7433−7447.

(3) Ribelli, T. G.; Lorandi, F.; Fantin, M.; Matyjaszewski, K. Atom Transfer Radical Polymerization: Billion Times More Active Catalysts and New Initiation Systems. *Macromol. Rapid Commun.* **2019**, *40*, 1800616.

(4) Corrigan, N.; Jung, K.; Moad, G.; Hawker, C. J.; Matyjaszewski, K.; Boyer, C. Reversible-Deactivation Radical Polymerization (Controlled/Living Radical Polymerization): From Discovery to Materials Design and Applications. *Prog. Polym. Sci.* **2020**, *111*, 101311.

(5) Whitfield, R.; Truong, N. P.; Messmer, D.; Parkatzidis, K.; Rolland, M.; Anastasaki, A. Tailoring Polymer Dispersity and Shape of Molecular Weight Distributions: Methods and Applications. *Chem. Sci.* **2019**, *10*, 8724−8734.

(6) Parkatzidis, K.; Wang, H. S.; Truong, N. P.; Anastasaki, A. Recent Developments and Future Challenges in Controlled Radical Polymerization: A 2020 Update. *Chem* **2020**, *6*, 1575−1588.

(7) Antonopoulou, M.-N.; Whitfield, R.; Truong, N. P.; Wyers, D.; Harrisson, S.; Junkers, T.; Anastasaki, A. Concurrent Control over Sequence and Dispersity in Multiblock Copolymers. *Nat. Chem.* **2022**, *14*, 304−312.

(8) Hawker, C. J.; Bosman, A. W.; Harth, E. New Polymer Synthesis by Nitroxide Mediated Living Radical Polymerizations. *Chem. Rev.* **2001**, *101*, 3661−3688.

(9) Nicolas, J.; Guillaneuf, Y.; Lefay, C.; Bertin, D.; Gigmes, D.; Charleux, B. Nitroxide-Mediated Polymerization. *Prog. Polym. Sci.* **2013**, *38*, 63−235.

(10) Allan, L. E. N.; Perry, M. R.; Shaver, M. P. Organometallic Mediated Radical Polymerization. *Prog. Polym. Sci.* **2012**, *37*, 127−156.

(11) Poli, R. A Journey into Metal−Carbon Bond Homolysis. *C. R. Chim.* **2021**, *24*, 147−175.

(12) Wayland, B. B.; Poszmik, G.; Mukerjee, S. L.; Fryd, M. Living Radical Polymerization of Acrylates by Organocobalt Porphyrin Complexes. *J. Am. Chem. Soc.* **1994**, *116*, 7943−7944.

(13) Debuigne, A.; Poli, R.; Jérôme, C.; Jérôme, R.; Detrembleur, C. Overview of Cobalt-Mediated Radical Polymerization: Roots, State of the Art and Future Prospects. *Prog. Polym. Sci.* **2009**, *34*, 211−239.

(14) Peng, C.-H.; Yang, T.-Y.; Zhao, Y.; Fu, X. Reversible Deactivation Radical Polymerization Mediated by Cobalt Complexes: Recent Progress and Perspectives. *Org. Biomol. Chem.* **2014**, *12*, 8580−8587.

(15) Kermagoret, A.; Debuigne, A.; Jérôme, C.; Detrembleur, C. Precision Design of Ethylene- and Polar-Monomer-Based Copolymers by Organometallic-Mediated Radical Polymerization. *Nat. Chem.* **2014**, *6*, 179−187.

(16) Debuigne, A.; Jérôme, C.; Detrembleur, C. Organometallic-Mediated Radical Polymerization of 'Less Activated Monomers': Fundamentals, Challenges and Opportunities. *Polymer* **2017**, *115*, 285−307.

(17) Demarteau, J.; Debuigne, A.; Detrembleur, C. Organocobalt Complexes as Sources of Carbon-Centered Radicals for Organic and Polymer Chemistries. *Chem. Rev.* **2019**, *119*, 6906−6955.

(18) Ayurini, M.; Chandler, P. G.; O'Leary, P. D.; Wang, R.; Rudd, D.; Milewska, K. D.; Malins, L. R.; Buckle, A. M.; Hooper, J. F. Polymer End Group Control through a Decarboxylative Cobalt-Mediated Radical Polymerization: New Avenues for Synthesizing Peptide, Protein, and Nanomaterial Conjugates. *JACS Au* **2022**, *2*, 169−177.

(19) Peng, C.-H.; Scricco, J.; Li, S.; Fryd, M.; Wayland, B. B. Organo-Cobalt Mediated Living Radical Polymerization of Vinyl Acetate. *Macromolecules* **2008**, *41*, 2368−2373.

(20) Liao, C.-M.; Hsu, C.-C.; Wang, F.-S.; Wayland, B. B.; Peng, C.-H. Living Radical Polymerization of Vinyl Acetate and Methyl Acrylate Mediated by Co(Salen*) Complexes. *Polym. Chem.* **2013**, *4*, 3098−3104.

(21) Wang, F.-S.; Lin, S.-H.; Zheng, G.-H.; Li, M.-H.; Cheng, Y.-C.; Peng, C.-H. Coordination of Azobisisobutyronitrile with Cobalt Complexes in Cobalt-Mediated Radical Polymerization Disclosed by Linear Correlation between the Equilibrium Constant and Half-Wave Potential. *Macromolecules* **2022**, *55*, 4276−4283.

(22) Zhao, Y.; Yu, M.; Fu, X. Photo-Cleavage of the Cobalt−Carbon Bond: Visible Light-Induced Living Radical Polymerization Mediated by Organo-Cobalt Porphyrins. *Chem. Commun.* **2013**, *49*, 5186−5188.

(23) Zhao, Y.; Yu, M.; Zhang, S.; Liu, Y.; Fu, X. Visible Light Induced Living/Controlled Radical Polymerization of Acrylates Catalyzed by Cobalt Porphyrins. *Macromolecules* **2014**, *47*, 6238−6245.

(24) Zhao, Y.; Yu, M.; Zhang, S.; Wu, Z.; Liu, Y.; Peng, C.-H.; Fu, X. A Well-Defined, Versatile Photoinitiator (Salen)Co−CO2CH3 for Visible Light-Initiated Living/Controlled Radical Polymerization. *Chem. Sci.* **2015**, *6*, 2979−2988.

(25) Liu, X.; Tian, L.; Wu, Z.; Zhao, X.; Wang, Z.; Yu, D.; Fu, X. Visible-Light-Induced Synthesis of Polymers with Versatile End Groups Mediated by Organocobalt Complexes. *Polym. Chem.* **2017**, *8*, 6033−6038.

(26) Demarteau, J.; Kermagoret, A.; German, I.; Cordella, D.; Robeyns, K.; De Winter, J.; Gerbaux, P.; Jerome, C.; Debuigne, A.; Detrembleur, C. Halomethyl-Cobalt(Bis-Acetylacetonate) for the Controlled Synthesis of Functional Polymers. *Chem. Commun.* **2015**, *51*, 14334−14337.

(27) Isayama, S.; Mukaiyama, T. A New Method for Preparation of Alcohols from Olefins with Molecular Oxygen and Phenylsilane by the Use of Bis(Acetylacetonato)Cobalt(II). *Chem. Lett.* **1989**, *18*, 1071−1074.

(28) Shevick, S. L.; Obradors, C.; Shenvi, R. A. Mechanistic Interrogation of Co/Ni-Dual Catalyzed Hydroarylation. *J. Am. Chem. Soc.* **2018**, *140*, 12056−12068.

(29) Waser, J.; Gaspar, B.; Nambu, H.; Carreira, E. M. Hydrazines and Azides via the Metal-Catalyzed Hydrohydrazination and Hydroazidation of Olefins. *J. Am. Chem. Soc.* **2006**, *128*, 11693−11712.

(30) Zhu, R. Emerging Catalyst Control in Cobalt-Catalyzed Oxidative Hydrofunctionalization Reactions. *Synlett* **2019**, *30*, 2015−2021.

(31) Chiang, L.; Allan, L. E. N.; Alcantara, J.; Wang, M. C. P.; Storr, T.; Shaver, M. P. Tuning Ligand Electronics and Peripheral Substitution on Cobalt Salen Complexes: Structure and Polymerisation Activity. *Dalton Trans.* **2014**, *43*, 4295−4304.

https://doi.org/10.1021/jacs.2c04655
J. Am. Chem. Soc. 2022, 144, 13311−13318